JOURNAL OF SOLID STATE CHEMISTRY **132,** 443–446 (1997)
ARTICLE NO. SC977535

LETTER TO THE EDITOR

First Direct Synthesis by High Energy Ball Milling of a New Lanthanum Molybdate

P. Lacorre[1] and R. Retoux

Laboratoire des Fluorures, UPRES-A CNRS 6010, Université du Maine, F-72085 Le Mans Cedex 9, France

Communicated by J. M. Honig July 1, 1997; accepted July 3, 1997

High energy ball milling of mixtures of lanthanum and molybdenum oxides led to the *in situ* formation of a series of lanthanum molybdates, with a La : Mo ratio of 1 : 1 and various Mo oxydation states, depending on the vial and reacting materials. Among these molybdates, one had only been prepared through fused salt electrolysis previously, and another was not known up to now. This illustrates the relevance of ball milling as a potentially fruitful method to prepare new oxide compounds. The space group and cell parameters of the new lanthanum molybdate have been determined using electron and X-ray diffraction.

Ball milling is widely used for mechanically alloying elementary metals, leading to the formation of metastable phases, or to the extension of miscibility domains (1). Such a mechanical process has recently been applied to elementary oxides, inducing redox reactions and phase transformations, usually toward high pressure forms. In some systems, ball milling of mixtures of elementary oxides has been shown to generate solid solutions, or already known ternary phases. For recent overviews on the topic, see for instance Refs. (2, 3) and references therein.

In this Letter, we report the first direct synthesis of a new lanthanum molybdate by high energy planetary ball milling of a mixture of $La_2O_3 + 2MoO_3$. Three different types of milling conditions and starting materials were tested, each of them leading to the formation of a different lanthanum molybdate phase with a La : Mo ratio close or equal to 1 : 1. Table 1 summarizes the three different processes used for these syntheses.

The resulting materials were analyzed by X-ray diffraction (Philips diffractometer), electron microscopy (Jeol 2010 microscope operated at 200 kV) in the diffraction, high resolution, and EDX analysis modes, and TGA measurement under flowing oxygen (Setaram TGA 92 thermoanalyzer).

X-ray diffraction patterns of the resulting materials are given in Fig. 1. Diffraction peaks are broader and smaller than those of the starting materials, indicating small particle sizes.

In the following, the materials resulting from each of the three milling processes are examined more thoroughly.

PROCESS A

The color of the resulting material is white. Its X-ray diffraction pattern corresponds to JCPDS file 28-0509 ascribed to $La_2Mo_2O_9$. This molybdate is signaled (4) to have the cubic symmetry ($a = 7.155$ Å), but its structure is unknown.

EDX analysis did not detect any Zr inside $La_2Mo_2O_9$ grains; only few grains, probably abraded from the vial, were shown to contain large amounts of zirconium. $La_2Mo_2O_9$ grains are rather large, a majority of them ranging in size between 100 and 500 nm and a few larger than 500 nm. The grains are usually poorly crystallized, with very disturbed shape and thickness, and they are built from multidomains. Thin amorphous regions have been observed at the domains edges.

$La_2Mo_2O_9$ is normally prepared by annealing a mixture of La_2O_3 and $2MoO_3$ in air at 500–800°C. We show here that it is possible to prepare this compound in the form of small particles by direct ball milling synthesis.

PROCESS B

The diffractogram of the resulting black phase corresponds to JCPDS file 35-1476 which is assigned to composition $La_2Mo_2O_7$ (from Ref. (5), space group *Pnnm*, $a = 6.034(1)$ Å, $b = 12.236(2)$ Å, $c = 3.888(1)$ Å).

[1]To whom correspondence should be addressed.

0022-4596/97 $25.00

TABLE 1

Process	Starting materials	Vial[a]/balls materials	Number of balls	Mass ratio[b]	Milling time (h)	Vial speed[c] (tr/min)	Resulting materials
A	$La_2O_3 + 2MoO_3$	ZrO_2	6	1:38	12	1384	$La_2Mo_2O_9$
B	$La_2O_3 + 2MoO_2$	WC	6	1:100	12	1384	$La_2Mo_2O_7$
C	$La_2O_3 + 2MoO_3$	WC	6	1:100	12	1384	New phase "$La_2Mo_2O_{8.5-\delta}$"

[a] Vials volume = 45 ml, balls diameter = 12 mm.
[b] Mass ratio = sample mass : total balls mass; for each process, the mass of starting materials was 1 g.
[c] Planetary mill (Frietsch Pulverisette 7) with 2 vials, the vials speed being twice the mill speed.

The grains morphology is basically the same as that of $La_2Mo_2O_9$ grains previously described, with size smaller than 500 nm. EDX analysis did not detect any tungsten within the crystallized or the amorphous parts of the grains.

$La_2Mo_2O_7$ had previously been prepared by molten salt electrolysis, as single crystals grown at the cathode from a melt of $Na_2MoO_4 + MoO_3 + La_2O_3$ (ratio 2.4 : 2.4 : 1.0) at 1070°C (5, 6). It is to be noted that several attempts, by other groups (6) and by the authors, to prepare this phase from powders under various conditions have been unsuccessful up to now. To our knowledge, this is the first time that $La_2Mo_2O_7$ is directly prepared as a powdered sample. This result emphasizes the possibilities offered by ball milling processes to stabilize oxide phases which normally can only be obtained under very specific conditions (here, from a melt in the presence of electric current).

PROCESS C

The material resulting from process C is black. Its X-ray diffraction pattern (Fig. 1C) does not appear to correspond to any known phase referenced in the JCPDS files. To our knowledge, this is the first time that a crystallized phase with a completely new structural arrangement resulting from ball milling of oxides is reported (Fig. 2).

The particles' shape is usually smooth, ovoid, or close to spherical, and their size is almost always smaller than 100 nm, with few exceptions up to 200 to 300 nm. Each particle consists of two distinct regions, as can be seen in Fig. 3a: a central, well-crystallized, and single-domain region, and a surrounding amorphous region. The thickness of this amorphous region can extend up to one-fourth to one-third of the total particle radius. The amorphous region is responsible for the undulated background observed in the X-ray diffraction patterns (see Fig. 1) and for the poor quality of the high resolution images, since it obviously surrounds completely the well-crystallized region. However, annealing of the resulting materials in an appropriate atmosphere induces the crystallization of this amorphous region, resulting in well-crystallized and single-domain particles, as can be seen in Fig. 3b. Correlatively, X-ray diffraction patterns of the annealed materials exhibit sharpened peaks on a flat background (Fig. 2d).

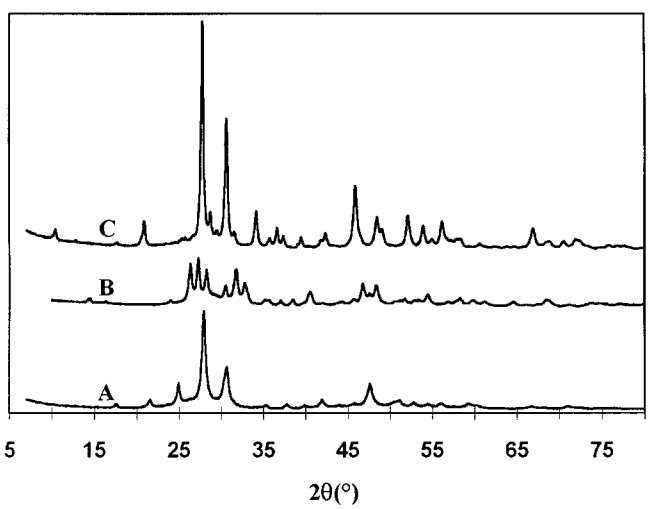

FIG. 1. X-ray diffraction patterns of the oxide phases resulting from process A ($La_2Mo_2O_9$), process B ($La_2Mo_2O_7$), and process C (new phase).

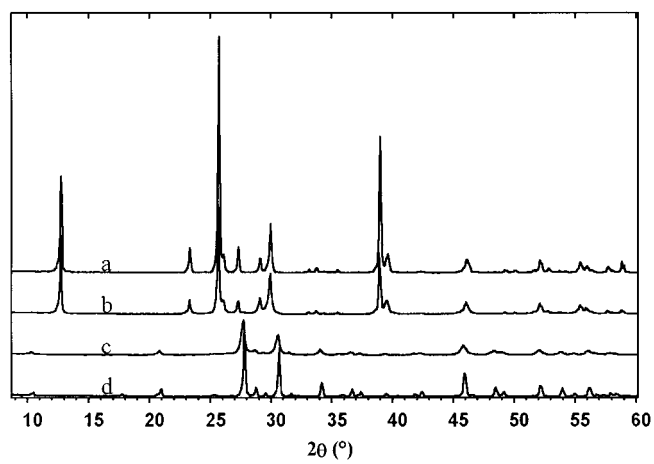

FIG. 2. X-ray diffraction patterns of the different phases present during process C: (a) starting materials $La_2O_3 + 2MoO_3$, (b) starting materials after 1 h ball milling with 3 WC balls, (c) resulting material after 12 h ball milling with 6 WC balls (new phase), and (d) new phase better crystallized after annealing in vacuum.

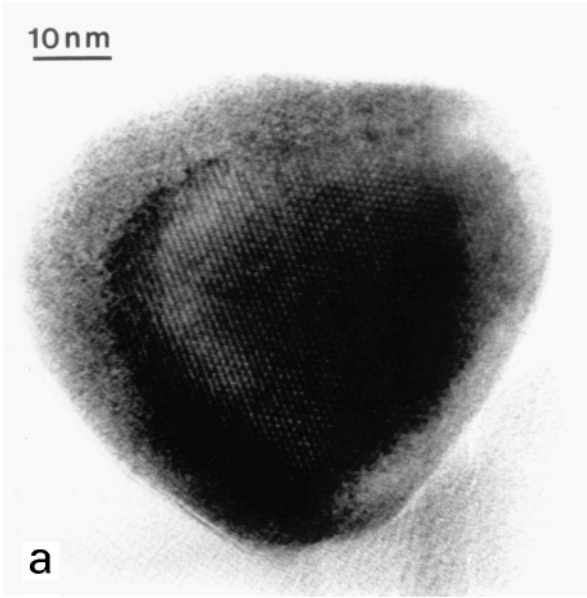

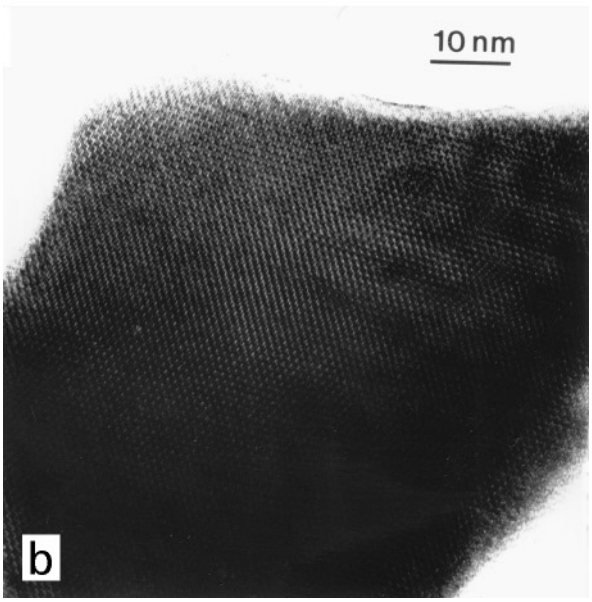

FIG. 3. Typical HREM images of: (a) a grain of the new lanthanum molybdate phase resulting from process C. Notice the central, single-domain crystallized part, surrounded by an amorphous matrix. (b) a grain of the same phase after annealing in vacuum.

From the above results, it seems evident that the vial material takes a crucial part in the stabilization of this phase, since milling of the same starting materials in a ZrO_2 vial does not lead to the same phase. However, it is not yet clear what the exact role of tungsten carbide is in the reaction. The change in the resulting compound from white in a ZrO_2 vial to black in a WC vial seems to show that molybdenum reduction occurred during reaction; this is a commonly observed phenomenon when oxides are ground in metallic vials (7). The reduction process has been confirmed by TGA measurement on the new phase under oxygen which shows a weight gain (see Fig. 4), the final oxidation product being mostly $La_2Mo_2O_9$. The deduced formula for the new phase is approximately $La_2Mo_2O_{8.5-\delta}$ (δ close to 0.07). Some similarities in the X-ray diffraction

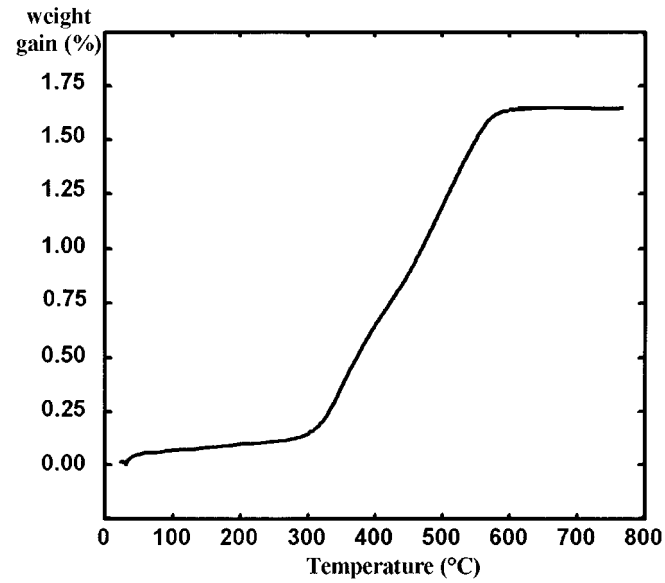

FIG. 4. TGA curve of the new phase (resulting from process C after recrystallization) under flowing oxygen (heating rate, 10°C/min).

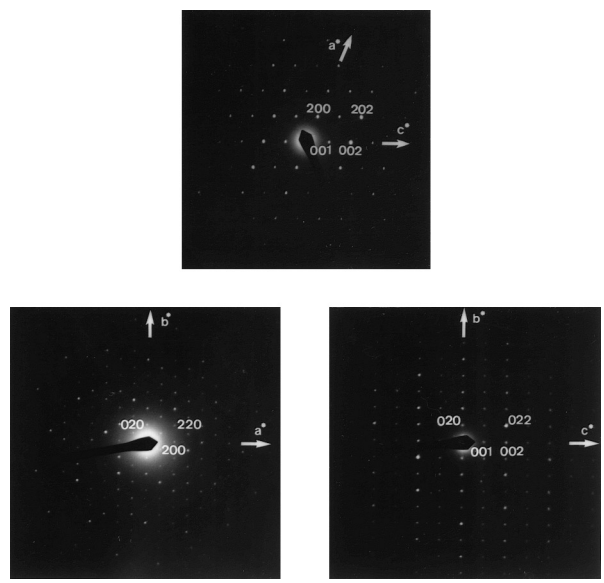

FIG. 5. [100], [010], and [001] electron diffraction patterns of "$La_2Mo_2O_{8.5-\delta}$." The conditions of systematic reflection deduced from several reciprocal lattice reconstructions are hkl: $h + k = 2n$, $h0l$: $h = 2n$, and $0k0$: $k = 2n$, involving the space group $C2/m$.

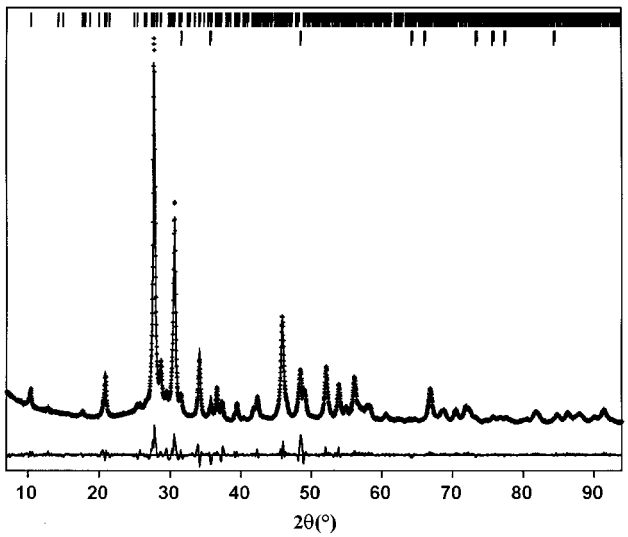

FIG. 6. Profile matching of the X-ray diffraction pattern of the new lanthanum molybdate resulting from process C, using space group $C2/m$ (cell parameters and reliability factors given in the text). The impurity phase is tungsten carbide from the vial and balls.

patterns of the two phases might be the sign of a resemblance of their crystal structures, one possibly being a reduced form of the other. However, the two phases do not appear to have the same symmetry, as will be seen below. Besides, the presence of some small impurity reflections in the X-ray diffraction pattern might indicate that the real stoichiometry of the new phase is slightly different from La : Mo = 1 : 1. In addition, small amounts of tungsten homogeneously distributed within the resulting materials particles have been detected by EDX analysis. Tungsten amounts to about 1 to 2% of the cation number of the particles. Its insertion in the crystal lattice might have some effect on the stabilization of the phase.

The electron diffraction study of the new phase allowed the determination of the space group ($C2/m$, see Fig. 5) and approximate cell parameters.

Refinement of the cell parameters was carried out using the program CELREF. Subsequently, a full pattern fit was undertaken on the as-prepared phase using the profile matching mode of the program FULLPROF. Figure 6 presents the observed, calculated, and difference patterns. The reliability factors are $R_p = 0.123$, $R_{wp} = 0.144$, $R_{exp} = 0.057$, $\chi^2 = 6.50$, $R_{Bragg} = 0.064$. Crystal cell parameters were determined to be $a = 10.5003(6)$ Å, $b = 16.982(1)$ Å, $c = 6.6218(4)$ Å, $\beta = 110.158(4)^\circ$. A crystal structure determination of this new phase is currently in progress.

In conclusion to this Letter, we want to point out the relevance of ball milling as a potentially fruitful method for preparing new oxides, as shown here on lanthanum molybdates. A convenient choice of the vial and balls material allows the stabilization of various oxidation states of the involved metals. A drawback could be the poor crystallinity of the phases thus obtained, but annealing in an appropriate atmosphere is likely to substantially improve it.

ACKNOWLEDGMENTS

The authors express special thanks to Dr. N. Randrianantoandro (Laboratoire de Physique de l'Etat Condensé, Université du Maine) for the access to the ball milling apparatus and for helpful discussions.

REFERENCES

1. J. J. De Barbadillo, *Key Eng. Mater.* **77,** 187 (1993).
2. S. Beguin-Colin, G. Le Caër, A. Mocellin, C. Jurenka, and M. Zandona, *J. Solid State Chem.* **127,** 98 (1996).
3. S. Beguin-Colin, F. Wolf, and G. Le Caër, *J. Phys. III Fr.* **7,** 473 (1997).
4. J. P. Fournier, J. Fournier, and R. Kohlmuller, *Bull. Soc. Chim. Fr.* 4277 (1970).
5. A. Moini, M. A. Subramanian, A. Clearfield, F. J. DiSalvo, and W. H. McCarroll, *J. Solid State Chem.* **66,** 136 (1987).
6. W. H. McCarrol, C. Darling, and G. Jakubicki, *J. Solid State Chem.* **48,** 189 (1983).
7. S. Beguin-Colin, G. Le Caër, M. Zandona, E. Bouzi, and B. Malaman, *J. Alloys Compd.* **227,** 157 (1995).